Regular Article

THROMBOSIS AND HEMOSTASIS

Red blood cells mediate the onset of thrombosis in the ferric chloride murine model

Justin D. Barr,[1] Anil K. Chauhan,[1] Gilbert V. Schaeffer,[2] Jessica K. Hansen,[3] and David G. Motto[1,2,4]

[1]Department of Internal Medicine, [2]Department of Anatomy and Cell Biology, University of Iowa Carver College of Medicine, Iowa City, IA; [3]Department of Biomedical Engineering, University of Iowa College of Engineering, Iowa City, IA; and [4]Department of Pediatrics, University of Iowa Carver College of Medicine, Iowa City, IA

Key Points

- The ferric chloride model does not result in endothelial denudation.
- In the ferric chloride model, platelets bind to endothelial-associated RBC-derived material rather than to the endothelial surface.

Application of ferric chloride ($FeCl_3$) to exposed blood vessels is widely used to initiate thrombosis in laboratory mice. Because the mechanisms by which $FeCl_3$ induces endothelial injury and subsequent thrombus formation are little understood, we used scanning electron and brightfield intravital microscopy to visualize endothelial damage and thrombus formation occurring in situ. Contrary to generally accepted belief, $FeCl_3$ does not result in appreciable subendothelial exposure within the time frame of thrombosis. Furthermore, the first cells to adhere to $FeCl_3$-treated endothelial surfaces are red blood cells (RBCs) rather than platelets. Energy dispersive x-ray spectroscopy demonstrated that ferric ions predominantly localize to endothelial-associated RBCs and RBC-derived structures rather than to the endothelium. With continuing time points, RBC-derived structures rapidly recruit platelets, resulting in large complexes that subsequently enlarge and coalesce, quickly covering the endothelial surface. Further studies demonstrated that neither von Willebrand factor nor platelet glycoprotein Ib-α receptor (GPIb-α) is required for RBCs to adhere to the endothelium, and that deficiency of GPIb-α greatly abrogated the recruitment of platelets to the endothelial-associated RBC material. These findings illuminate the mechanisms of $FeCl_3$-mediated thrombosis and reveal a previously unrecognized ability of RBCs to participate in thrombosis by mediating platelet adhesion to the intact endothelial surface. (*Blood*. 2013;121(18):3733-3741)

Introduction

Murine vascular thrombosis models are used widely to (1) characterize the phenotypes of animals with targeted gene deletions and transgenic insertions, (2) better describe the mechanisms of action of known hemostatic and antithrombotic agents, and (3) generate preclinical data for potential therapeutic agents.[1-3] As these types of physiologic studies are optimally performed in the context of the whole organism, the use of vascular thrombosis models in laboratory mice has become essential in hemostasis and thrombosis research.

Experimental thrombosis in mice is generally induced in exposed vessels by 1 of 3 methods: (1) applying ferric chloride ($FeCl_3$), (2) directly inducing with a laser, or (3) indirectly inducing with a laser to excite photoreactive chemicals previously introduced into the circulation (eg, rose bengal). Subsequently, thrombus formation either is followed visually by intravital microscopy or the time to occlusion is determined with a Doppler flow probe. These experiments are typically performed at sites accessible to flow probe placement (eg, the common carotid artery or jugular vein) or microscopy (eg, mesenteric or cremasteric arterioles and venules).

Of these models, the most common has become $FeCl_3$-induced injury of the common carotid artery,[4] likely secondary to its relative ease of implementation, low cost, and nonrequirement of a specialized laser. Application of $FeCl_3$ is thought to cause rapid denudation of the endothelial surface, with concomitant exposure of the subendothelial matrix.[5,6] The uncovering of prothrombotic molecules such as collagen and tissue factor is then believed to result in the recruitment of platelets and their subsequent activation, followed by activation of the coagulation cascade.[4]

Relative to the number of studies using $FeCl_3$-induced vascular injury to investigate the biology of hemostasis and thrombosis, there have been comparatively few mechanistic studies into this model.[5-8] Therefore, to investigate the mechanisms of $FeCl_3$-induced endothelial injury and thrombus formation in greater detail, we used scanning electron microscopy (SEM) and brightfield intravital microscopy to visualize endothelial damage and thrombus formation that occur in situ. These studies resulted in several novel and unexpected findings regarding the nature of $FeCl_3$-induced injury and the induced mechanisms of thrombosis in this widely used vascular injury model.

Materials and methods

Animals

C57BL/6 mice from Jackson Laboratories were used to maintain a breeding colony for all wild-type mice used. von Willebrand factor (VWF)-deficient[9]
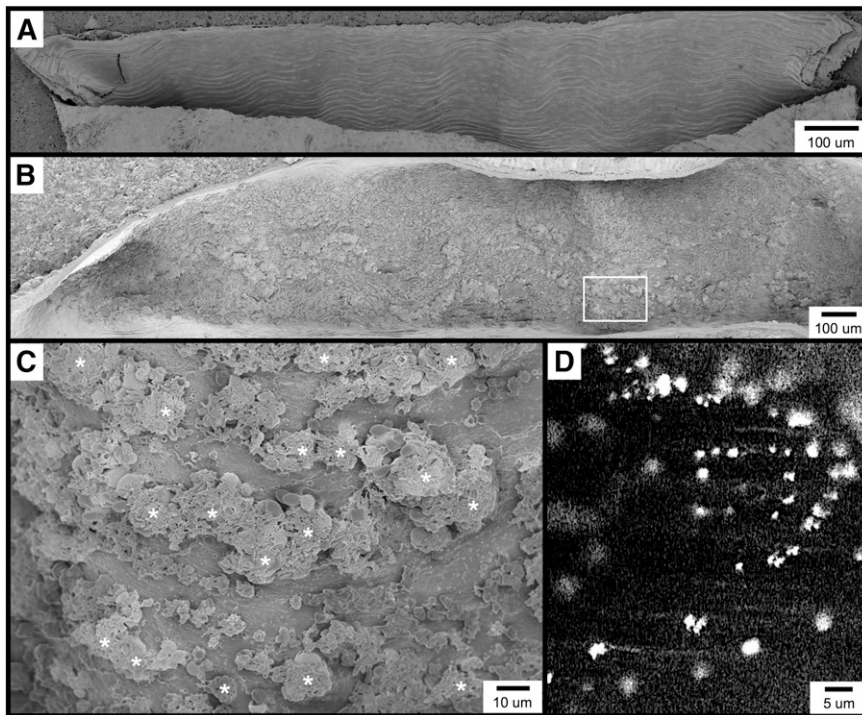
Figure 1. Visualization of the carotid artery endothelial surface by SEM. (A) The image shows a longitudinal section from an untreated mouse, approximately 1.5 mm long. (B-C) The images are of the carotid artery 1 minute following $FeCl_3$ application, visualized by SEM. Thrombotic material can be observed covering much of the endothelial surface. Higher magnification of the area from (B, box) is shown in (C). (D) The fluorescent intravital microscopy image shows $FeCl_3$-induced thrombosis in the mouse carotid artery. Platelets were observed to bind in clusters rather than discretely. The time frame is approximately 30 seconds following the application $FeCl_3$. *, platelet clusters (not all are marked).

and glycoprotein Ib-α (GPIb-α)–deficient/IL-4R-α transgenic[10] mice were gifts of Denisa Wagner and Jerry Ware, respectively; both lines are maintained on a C57BL/6 background in our laboratory. Mouse ages were eight to 12 weeks for the SEM studies and 4 to 6 weeks for the intravital studies. All procedures were approved by the Animal Use and Care Committee of the University of Iowa (Iowa City, IA) before implementation.

Important note about SEM sample handling, preparation, and interpretation

We have found that meticulous technique during all phases of handling and preparation is necessary to minimize experimental artifacts and to result in samples suitable for interpretation. For example, with improper preparation and handling, it is not uncommon to find endothelial denudation with subendothelial exposure in *untreated* samples. Furthermore, the images presented here (unless otherwise specified) are highly representative of large numbers of possible examples.

$FeCl_3$, mechanical injury, and carotid artery preparation

Mice were anesthetized with sodium pentobarbital (80 to 100 mg/kg intraperitoneal). A 1×5–mm strip of filter paper (Whatman no. 1) saturated with 10% ferric chloride (0.617 M) was applied directly to the previously exposed right common carotid artery. At the desired time, the strip was removed and the mice were perfused through the previously exposed left ventricle with phosphate-buffered saline (PBS) followed by fixative (2.5% glutaraldehyde; 3.2% paraformaldehyde in PBS, pH 7.4 Electron Microscopy Sciences [EMS], Hatfield, PA). Vessels were excised and bathed overnight in the same fixative. Mechanical injury was performed analogously, with $FeCl_3$ application replaced with careful pinching of the exposed vessel for exactly 3 seconds with microsurgical forceps (no. 11063-07, Fine Science Tools, Foster City, CA), using pressure just sufficient to completely oppose the angles of the forceps.

SEM sample preparation and imaging

Excised vessels were manually sectioned with an unused, ethanol-cleaned razor blade washed with PBS, and then postfixed with 1% osmium tetroxide for 1 hour (EMS). Following a second wash with PBS, the samples were dehydrated through an ethanol dilution series before being either chemically dried with hexamethyldisilazane (EMS) or subjected to critical point drying. Sputter coating was done with ~10 nm gold-palladium (EMS). Imaging was performed in the Central Microscopy Research Facility at the University of Iowa (Iowa City, IA) with either a Hitachi S-4800 FE-SEM or a Hitachi S-3400N VP-SEM in conjunction with a Bruker AXS energy dispersive x-ray spectroscope.

In vitro RBC adhesion studies

Confluent human umbilical vein endothelial cells (HUVECs) grown on coverslips were assembled into a parallel-plate flow chamber (no. 64-1685, Warner Instruments, Hamden, CT) and subsequently perfused with washed human RBCs (de-identified samples from the University of Iowa Blood Bank) suspended at a hematocrit of 12.5% in either PBS (pH 6.5) or in PBS plus 250 μM $FeCl_3$ (pH 6.5) at ~2.5 dyne/cm^2 for 10 minutes. The chamber was subsequently perfused with PBS to wash out nonadherent cells. Images were collected, and analyses were performed as indicated.

Platelet preparation and labeling, carotid intravital microscopy, and mesenteric intravital microscopy

Platelet preparation and labeling as well as microscopy were performed as described previously in Chauhan et al[11] and Megens et al [12] and in the supplementary methods.

Results

Figure 1A shows an example of carotid artery endothelium from an untreated, wild-type C57BL/6 mouse (for all SEM micrographs, the direction of flow is from right to left in all horizontally oriented images, and from top to bottom in all vertically oriented images). Individual endothelial cells can be clearly discerned and observed to be aligned along the long axis of the blood vessel. A single endothelial cell measuring approximately 40×10 μm is shown in supplementary Figure 1A. The surface of this cell when viewed at higher magnification (supplementary Figure 1B) reveals a

fenestrated appearance of the plasma membrane along with characteristic membrane appendages. Very few blood cells are found to be adherent to the uninjured/resting endothelium, although rare individual platelets, leukocytes, and erythrocytes can be observed.

FeCl$_3$-induced vascular injury results in the rapid formation of platelet-rich thrombi, which in the common carotid artery typically become occlusive within approximately 7 to 10 minutes when 10% FeCl$_3$ is used (and within 7 minutes under the conditions of this study).[4] With SEM, we found that within 1 minute of FeCl$_3$ application, the endothelial surface appears nearly covered with thrombotic material (Figure 1B). Although platelets can be identified, they appear to be binding in clusters rather than adhering discretely to the endothelial surface (Figure 1C). Consistent with this observation, intravital microscopy of the common carotid artery similarly demonstrated fluorescent platelets binding in clusters considerably larger than a single platelet (Figure 1D and supplementary Movie 1). Similar platelet clusters were also observed in both mesenteric arterioles and venules following FeCl$_3$ application (not shown).

It has been reported and widely referenced that FeCl$_3$ treatment results in endothelial cell denudation and exposure of the subendothelial matrix.[5-7,13] However, examination of multiple micrographs of the FeCl$_3$-treated carotid surface at time points following the onset of thrombosis revealed the endothelial surface to be intact (supplementary Figure 1C), with its characteristic appendages and fenestrated appearance remaining visible at higher magnification (supplementary Figure 1D). FeCl$_3$ treatment does, however, result in the appearance of large numbers of "blisterlike" structures on the endothelial surface (supplementary Figure 1C-D), the origin of which will be discussed below.

The appearance of the FeCl$_3$-treated endothelium is distinct and clearly differentiated from endothelial denudation and subendothelial exposure induced by mechanical trauma (supplementary Figure 1E). Furthermore, upon true endothelial denudation, platelets bind to the exposed subendothelium and spread with a characteristic appearance (supplementary Figure 1F). As described below, such platelet adhesion and spreading was not observed following FeCl$_3$ application. These findings revealed that FeCl$_3$ application does not result in endothelial denudation within the time frame of the onset of thrombosis, and they suggest that thrombosis in this model therefore must be driven initially by a process distinct from platelet binding to the exposed subendothelium.

Further examination of the thrombotic material occurring within 1 minute of FeCl$_3$ application revealed the widespread occurrence of several cell types and structures, including elongated red blood cells (RBCs; Figure 2A), RBC clusters (Figure 2B), spherical structures (Figure 2C [also Figure 2A,E]), spherical structures covered with smaller, rough-appearing bodies (Figure 2D [also Figure 2A,C,E]), and complexes exhibiting a considerable amount of amorphous-appearing material (Figure 2E). Although platelets are present in several of these micrographs, they were not observed to be adherent to the endothelial surface but rather to be binding to the elongated RBC clusters (Figure 2B), spherical structures (Figure 2A, C), and amorphous material (Figure 2E).

To elucidate the cellular origin of the spherical structures observed following FeCl$_3$ application (eg, Figure 2C), we obtained high-magnification images of a standard-appearing RBC (supplementary Figure 2A), an elongated RBC (supplementary Figure 2B), and a spherical structure (supplementary Figure 2C). As shown, all 3 exhibited a nearly identical surface appearance (supplementary Figure 2D-F), which differs considerably from that of
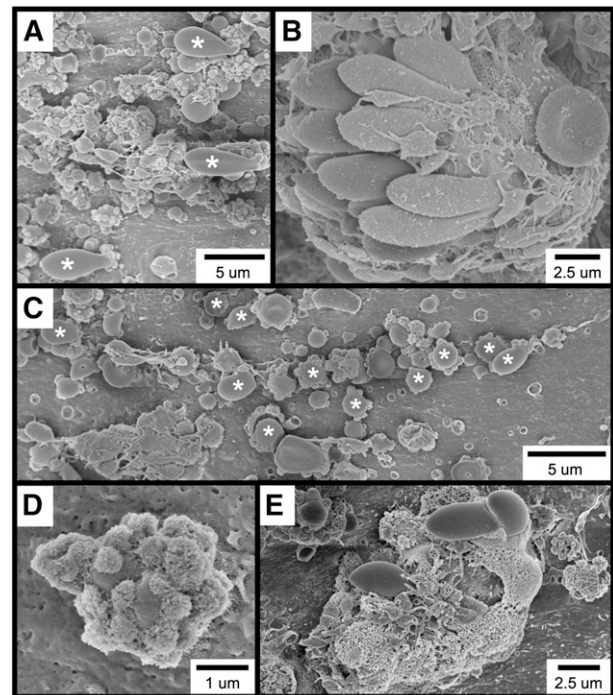

Figure 2. SEM visualization of thrombotic material in the mouse carotid artery induced by FeCl₃ application. The figure shows (A) elongated RBCs (asterisks); (B) an RBC cluster; (C) spherical structures (asterisks; not all are labeled); (D) a spherical structure covered with smaller, rough-appearing bodies; and (E) complexes composed of rough and amorphous-appearing material. The time course was 1 minute after FeCl₃ application for all samples.

FeCl$_3$-treated endothelium (supplementary Figure 2G-H). These observations suggest that these spherical structures are derived from RBCs rather than representing endothelial-derived ferric ion–containing exocytic bodies.[7] Thus, henceforth these structures will be referred to as "RBC fragments."

To directly visualize the adhesion of RBCs and the formation of RBC fragments following FeCl$_3$ application, we used brightfield intravital microscopy of mesenteric vessels (supplementary Movie 2). As shown, within approximately 30 seconds of FeCl$_3$ application, RBCs were observed to adhere to the endothelial surface of mesenteric venules, both singly and multiply, often forming large multicellular clusters (Figure 3A-D, upper panels). Identical findings were also obtained in mesenteric arterioles (not shown). SEM imaging of analogous structures that formed in the FeCl$_3$-treated carotid artery is shown in Figure 3A-D, lower panels.

Further examination of RBC adhesion to the endothelial surface by intravital microscopy revealed that, following binding, a dense ringlike structure becomes visible within the adherent RBC (Figure 3E). Under in vivo conditions, adherent RBCs and RBC fragments appear to be fixed to the endothelial surface at these ringed structures, which therefore seem to represent what we term "firm adhesion points" between RBC-derived structures and the endothelium. Experiments performed in mice injected with rhodamine 6G (to label platelets and leukocytes) demonstrated that the adhesion of RBC-derived structures at these points is not mediated by platelets or leukocytes serving as an intermediary binding site (Figure 3F-G), which is further supported by visualization with SEM (Figure 3H-I).

We next performed frame-by-frame video analyses of FeCl$_3$-induced RBC adhesion, which revealed the formation of elongated RBCs and RBC fragments (Figure 4 and supplementary Movie 3).
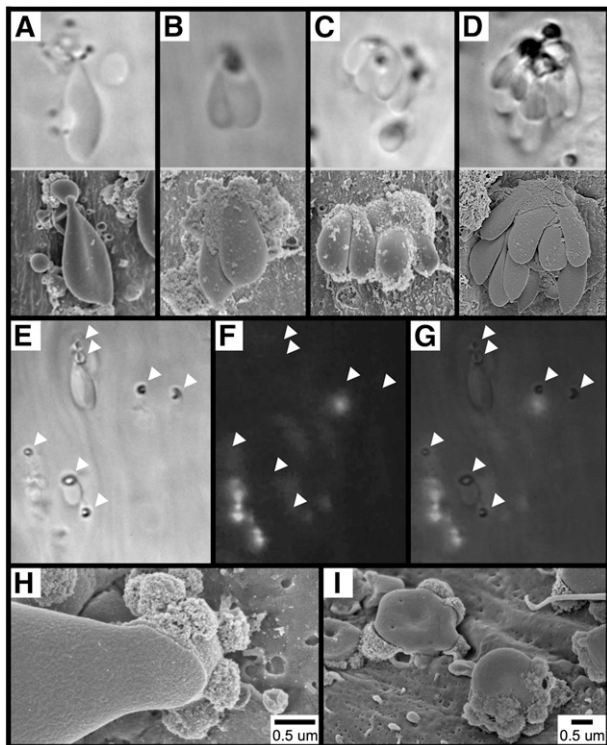
Figure 3. Adhesion of RBCs to the endothelial surface following FeCl₃ application. The images in (A-D, upper panels) show the mesenteric venule with visualization by brightfield intravital microscopy (original magnification ×100). The time course was between 1 and 5 minutes after FeCl₃ application. The images in (A-D, lower panels), show the carotid artery with visualization by SEM. The time course was 1 minute for (A-C) and 90 seconds for (D) after FeCl₃ application. Note that for intravital microscopy, the angle of observation is from "below," looking up the "underside" of the structures, while the angle of observation for SEM is from "above," looking down at the "top" of the structures. The images in (E-I) show that the adhesion of RBCs to the endothelial surface is not mediated by platelets or leukocytes. Brightfield (E), fluorescent (F), and merged (G) intravital microscopy imaging was performed on FeCl₃-induced RBC adhesion in murine mesenteric venules (rhodamine 6G injected). Arrowheads indicate the locations of firm adhesion points. The time course is approximately 3 minutes following FeCl₃ application. (H-I) SEM imaging shows an elongated RBC (H) and RBC fragments (I) directly adherent to the carotid endothelial surface 1 minute following FeCl₃ application.

In the first representative image (Figure 4A), a pair of RBCs is initially observed associated with the endothelial surface (arrows, panel Ab). After approximately 0.6 seconds, a firm adhesion point is visible within 1 of the RBCs (black arrow, panel Ac), along with a portion of this RBC becoming elongated in the direction of flow (white arrow, panel Ac). With later time points, the elongated segment appears to be attached to (or near) the firm adhesion point (white arrow, panel Ad). Subsequently, the elongated portion separates from the adhesion point (panel Ae), leaving an RBC fragment associated with the endothelial surface (black arrow, panel Af). Additional examples demonstrated a similar sequence of events (Figure 4B-C) and that firm adhesion points can be visualized within as little as 0.06 to 0.12 seconds following adhesion (panel Bc and panel Cb).

Further analyses revealed that many FeCl₃-induced RBC adhesion events occur quite transiently, and they do not result in the formation of a firm adhesion point (supplementary Figure 3). In the first example (supplementary Figure 3A), 2 RBCs adhere to the endothelial surface and become elongated in less than 0.03 seconds (supplementary Figure 3A, panel b). Subsequently, these cells move a small distance in the direction of blood flow (supplementary Figure 3A, panels c-e)**,** before dislodging from the endothelium within

0.15 seconds of their initial adhesion (supplementary Figure 3A, panel f). In the second example (supplementary Figure 3B), 2 RBCs are associated with the endothelial surface for less than 0.06 seconds total (supplementary Figure 3B, panels b-c). These findings demonstrated that transient RBC adhesion events do not result in the formation of any material visible by brightfield intravital microscopy, and that FeCl₃-induced, stable RBC adhesion to the endothelial surface is associated with the formation of firm adhesion points.

However, as described above, FeCl₃ application does result in the appearance of large numbers of blisterlike structures on the endothelial surface (supplementary Figure 3C). Further analyses demonstrated that these structures do not appear to represent the remnants of exocytic vesicles, as intact endothelium can still be visualized within their borders (supplementary Figure 3D). Rather, these structures, which we have termed "endothelial blisters," appear to represent material resulting from transient cellular binding events. Indeed, the adhesion of individual RBCs to the endothelium can result in structures resembling endothelial blisters (supplementary Figure 3E-F).

Further investigation of the rough-appearing material often associated with RBC fragments or the endothelial surface (eg, Figure 2D) revealed that these structures resemble the adhesion points of elongated RBCs associated with RBC fragments (supplementary Figure 4). Thus, we hypothesized that these rough-appearing structures represent the remnants of RBCs that had transiently bound to, and subsequently separated from, adherent RBC fragments. Indeed, frame-by-frame analysis of brightfield intravital microscopy (supplementary Figure 4D and supplementary Movie 4) demonstrated that, following FeCl₃-exposure, RBCs can transiently adhere to endothelial-associated RBC fragments, with distinct structures becoming visible at the point of attachment.

Together, these observations demonstrated that the rough-appearing structures observed bound to endothelial-associated RBC fragments and to the endothelial surface represent remnants of transiently adherent RBCs. Because of their appearance by SEM, these structures henceforth will be referred to as "rough bodies."

Although rough bodies represent fragments of adherent RBCs, these structures appear by SEM to be phenotypically distinct from RBCs. We hypothesized that this surface phenotype change may be brought about by the action of iron (Fe) ions present at the site of injury. To investigate this hypothesis, we performed energy dispersive x-ray spectroscopy (EDS) imaging of FeCl₃-treated murine carotid artery sections. Shown by standard SEM is an endothelial-associated RBC fragment coated with rough bodies and a single attached elongated RBC (supplementary Figure 5A). The same structures were then visualized with an EDS-equipped scanning electron microscope and displayed with and without the Fe signal (supplementary Figure 5B-C). As shown, iron molecules are detected both in the endothelial-associated RBC fragment and in the rough bodies but not in the elongated RBC. Interestingly, neither the endothelium nor the endothelial blisters return a strong Fe signal. Further imaging demonstrated that surface-associated RBC fragments and rough bodies consistently appear positive for high concentrations of iron molecules following FeCl₃ exposure, while platelets and elongated RBCs generally do not (supplementary Figure 5D-E).

We next investigated in more detail the amorphous-appearing material observed by SEM to be present in many endothelial-associated structures following FeCl₃ exposure (eg, Figure 2E). Imaging of multiple examples of these structures revealed that this rough material represents RBCs in various stages phenotypic

Figure 4. RBC fragment formation in mesenteric venules visualized by brightfield intravital microscopy. Elapsed times from the initial frames (panels a) are as indicated (seconds). For the example shown in (A), 2 RBCs (Ab, arrows) become associated with the endothelial surface; a firm adhesion point becomes visible within 1 of the RBCs (Ac, black arrow), with this RBC becoming elongated in the direction of flow (Ac, white arrow); the elongated RBC appears to be anchored to the firm adhesion point (Ad, white arrow); the elongated RBC breaks free from the firm adhesion point (Ae, white arrow); and the RBC fragment is left associated with the endothelial surface (Af, black arrow). (B-C) The black arrows indicate the firm adhesion point, and the white arrows indicate the adherent RBC fragment.
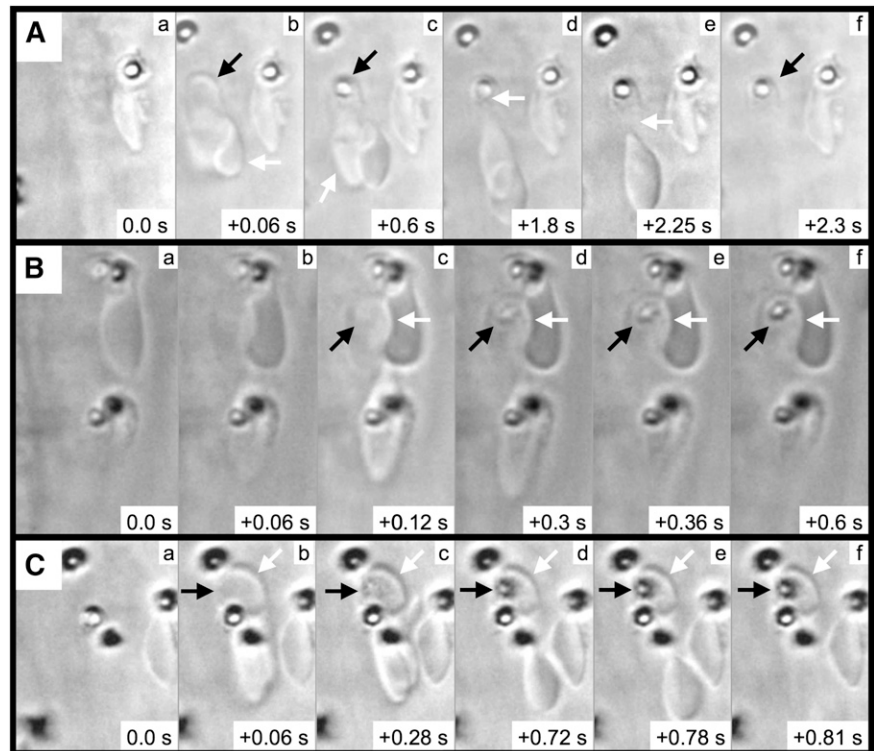
change (supplementary Figure 6A-C). Further analysis of these structures by EDS imaging demonstrated rough material to be strongly positive for iron content (supplementary Figure 6D-E). Thus, similar to rough bodies and endothelial-associated RBC fragments, Fe ions present at the site of application may result in the formation of rough material from adherent RBCs and RBC-derived structures.

As discussed above, it is often described that FeCl₃-induced vascular injury results in the formation of platelet-rich thrombi at the site of application. However, our observations demonstrated that RBCs are the first cells to adhere to the endothelium following FeCl₃ application. Regarding platelet recruitment, the examination of multiple examples of FeCl₃-treated vessels revealed that platelets predominantly adhere to endothelial-associated RBC-derived structures rather than to the endothelial surface (Figure 5). Additionally, composite images of large sections of FeCl₃-treated endothelium often fail to reveal even a single platelet directly adherent to the endothelial surface (supplementary Figure 7).

Further observations revealed that platelet binding to RBC-derived material often resulted in the generation of large platelet-RBC complexes, which can form quite rapidly (Figure 6A-F and supplementary Movie 5). With continuing time points, these large platelet-RBC complexes enlarge and coalesce, nearly covering the entire endothelial surface within 4 minutes of FeCl₃ application (Figure 6G-I). Examination of small areas devoid of thrombotic material revealed that the endothelial surface continues to be intact at this 4-minute time point (supplementary Figure 8A-B). Furthermore, examination of samples 10 minutes following application of FeCl₃ revealed an intact endothelial surface adjacent to the thrombus (supplemental Figure 8C).

To begin to investigate the mechanisms underlying FeCl₃-induced RBC adhesion and platelet recruitment, we performed SEM imaging of FeCl₃-treated carotid artery sections from mice lacking either VWF or the extracellular domain of GPIb-α. As shown, RBC-derived material is visible in samples from both types of mice, demonstrating that neither VWF (Figure 7A) nor GPIb-α (Figure 7B) is required for FeCl₃-induced RBC adhesion to the endothelial surface. Interestingly, platelet recruitment was greatly abrogated in mice deficient for GPIb-α, with only occasional platelets visible that were adherent to RBC-derived material (Figure 7B). In contrast, deficiency of VWF did not affect the binding of platelets to the endothelial-associated RBC material (Figure 7A). However, a comparison of concurrent samples from wild-type mice demonstrated that a deficiency of VWF does abrogate the further recruitment of platelets to the already established platelet-RBC complexes, resulting in a slower rate of thrombus formation (compare Figure 7A with Figure 6I). Finally, FeCl₃ is able to induce the adhesion of washed human RBCs to cultured human endothelial cells under flowing conditions in vitro (including the formation of RBC clusters), demonstrating that RBC-endothelial cell interaction can occur directly, in the absence of additional molecules (Figure 7C-E). Preliminary SEM imaging demonstrated that the adhesion point between RBCs and HUVECs in vitro resembled the rough bodies observed in vivo to mediate the binding of some RBCs with both the endothelial surface and with other RBCs (not shown).

Discussion

Interestingly, it was on the basis of SEM imaging that the first study to describe FeCl₃-induced experimental thrombosis (which was performed in the rat common carotid artery) concluded that FeCl₃ application results in (1) endothelial denudation and (2) adhesion of platelets to the exposed subendothelium.[5] However, a review of the images from this report suggested that, secondary to the quality of the SEM imaging available at the time of the
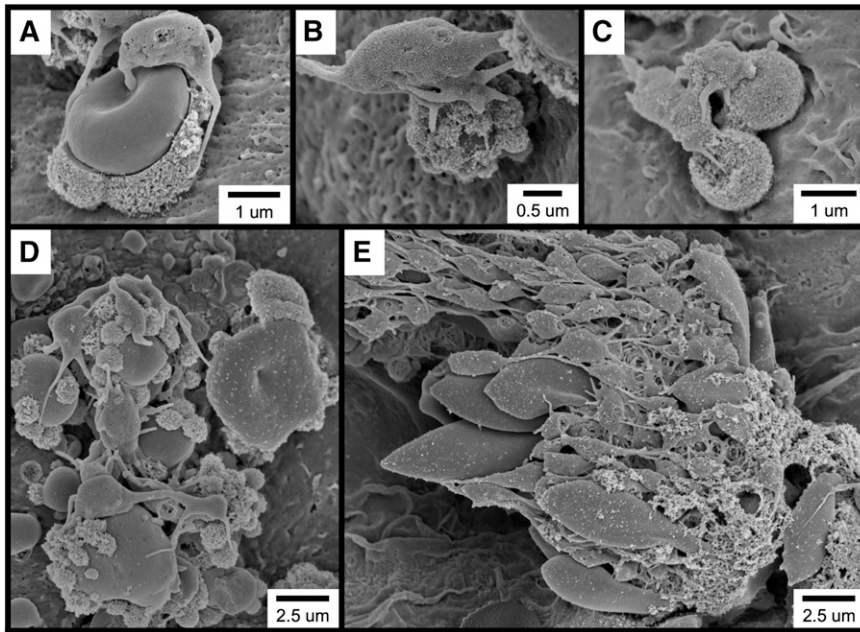
Figure 5. Following FeCl$_3$ application, platelets bind to RBC-derived structures rather than to the intact endothelial surface. (A-E) SEM visualization shows platelets binding to RBC-derived structures. The time course was 1 minute following FeCl$_3$ application for all samples.

study, both conclusions may have been reached erroneously. For example, the image from Kurz et al[5] describing endothelial denudation does not appear to be of sufficient quality to permit the differentiation of intact endothelium from exposed subendothelium, as we are able to do in this study.

The second study often referenced as describing FeCl$_3$-induced endothelial denudation reaches this conclusion based on decreased anti-VWF immunohistochemical staining in FeCl$_3$-treated mesenteric arteriolar cross sections.[6] Interestingly, a ring of positive VWF staining remains visible in the FeCl$_3$-treated sample from this important study, which the authors speculated could represent subendothelial VWF or plasma VWF deposition. However, in light of our findings, an alternative interpretation is that the persistence of anti-VWF staining following FeCl$_3$ application could indicate continued integrity of the endothelial cell layer.

In 2011, Eckly et al[7] investigated mechanisms underlying FeCl$_3$-induced arterial thrombosis using several techniques, including SEM and transmission electron microscopy (TEM). Interestingly, and consistent with our findings, these investigators demonstrated that, following FeCl$_3$ application, the internal elastic lamina remained intact, without exposure of the smooth muscle and deep adventitial collagen layers. However, in contrast to our
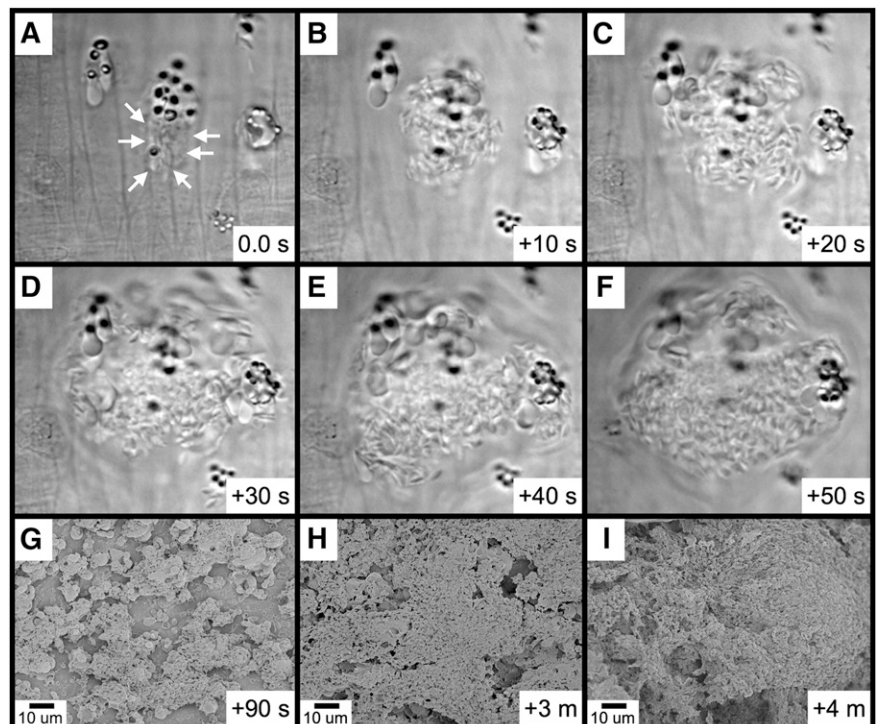
Figure 6. Rapid platelet aggregation on RBC-derived material visualized by brightfield intravital microscopy and SEM. (A-F) The elapsed time from the initial frame (A) is as indicated (seconds). (A) Platelets were observed binding to a group of RBC fragments (arrows). (B-F) Rapid platelet aggregation results in the formation of a large platelet complex. (G-I) Continued platelet aggregation following FeCl$_3$ application was visualized by SEM. The time course after FeCl$_3$ application is indicated in the panels.
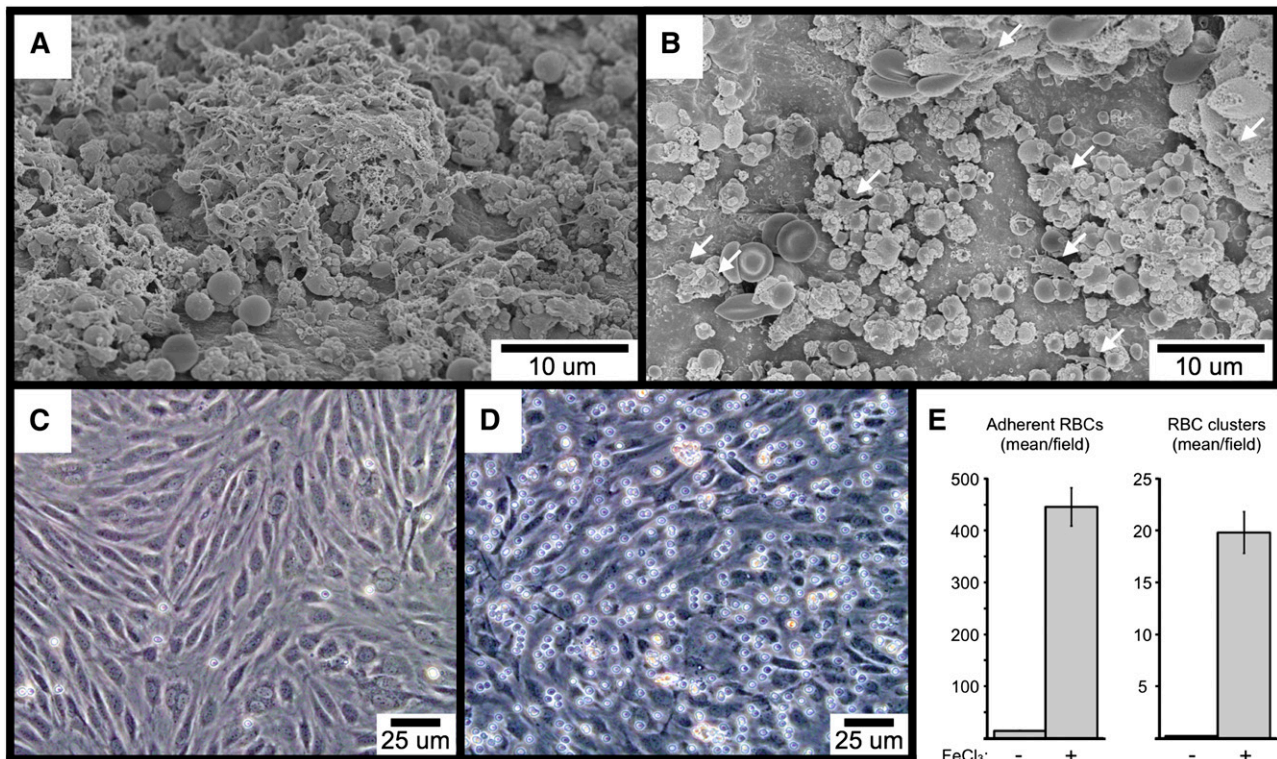
Figure 7. SEM visualization of carotid artery FeCl₃-induced thrombosis in VWF-deficient (A), and GPIb-α extracellular domain–deficient mice (B). The few platelets in (B) are indicated with arrows. The time course is 4 minutes after FeCl₃ application for both samples (A-B). (C-E) The images demonstrate FeCl₃-induced adhesion of washed human RBCs to cultured HUVECs under flow. (C) shows the buffer-only control, and (D) the buffer plus FeCl₃. The graph in (E) shows the quantitation of adherent RBCs and RBC clusters from 4 independent experiments, with a minimum of 5 random ×20 fields per experiment. Three or more RBCs together were considered a cluster. The error bars represent the standard error of the mean.

results, Eckly et al[7] also reported that FeCl₃ induces endothelial denudation. We believe this discrepancy most likely stems from differences in the techniques used in the 2 studies. Eckly et al[7] used TEM to visualize a cross section of the FeCl₃-treated murine common carotid artery and demonstrated approximately 10 μm of partially disrupted endothelial surface. However, as individual murine carotid endothelial cells measure approximately 10 × 40 μm, this cross-sectional micrograph represents a comparatively small area. In the current study, we used SEM to visualize much larger areas (eg, supplementary Figure 7), which represent 0.02 mm² of FeCl₃-treated endothelial surface. Additionally, it is possible that the physical act of cross sectioning for TEM could result in scattered artifactual disruption of the thin (<1 μm) endothelial surface, which is not an issue with longitudinal sectioning and SEM. Thus, we believe that our finding that the endothelial surface remains intact following FeCl₃ application extends the important observations of Eckly et al,[7] and together these studies demonstrate the surprising lack of collagen exposure in this model.

A clear corollary to this important finding is that if the endothelial surface remains intact following FeCl₃ application, then thrombosis must be initiated by a process distinct from platelet binding to the exposed subendothelium. Surprisingly, further investigation revealed that platelets are not even the first cells recruited to the site of FeCl₃ application. Rather, we demonstrated that RBCs are the initial cells to adhere to the FeCl₃-treated endothelial surface, and it is these RBCs (and RBC-derived material) to which platelets are subsequently recruited and thrombosis is initiated. Interestingly, several previous investigations have described the presence of RBCs and/or RBC fragments associated with the endothelial surface following FeCl₃ application but without functional implication regarding platelet binding.[5,7,14] In the current study, we confirmed and extended these earlier observations by describing the functional thrombotic consequences of RBC binding to the endothelial surface.

Many interactions of RBCs with the endothelial surface are transient, and they result in the formation of structures on the endothelial surface that we have termed endothelial blisters. Whether these structures are composed of material derived from endothelial cell membranes, RBC membranes, or a combination of both is unclear. Although endothelial blisters are highly characteristic of the FeCl₃-treated endothelial surface, the vast majority are not observed to be associated with any other cells or material, and thus are unlikely to be of functional significance.

In contrast, circulating RBCs also form stable associations with the endothelial surface, and it is these adhesion events that ultimately lead to the recruitment of platelets. Once stably associated with the endothelial surface, RBCs elongate in the direction of blood flow, appearing to be anchored to the endothelium at dense and often ringlike structures that we have termed firm adhesion points, which are visible by intravital microscopy. Firm adhesion points are not well visualized by SEM secondary to the overhead angle of observation. In most cases, stably associated RBCs partially break free from the firm adhesion point, leaving an RBC fragment (which is usually spherical) bound to the endothelial surface. Similar to endothelial blisters, RBC fragments are found in large numbers on the FeCl₃-treated endothelial surface.

In addition to the endothelial surface, circulating RBCs can also bind directly to surface-associated RBC fragments. Similar to RBCs binding to the endothelial surface, RBCs adhering directly to RBC fragments also elongate in the direction of flow, and they

appear to be anchored at a single point of contact. Additionally, and also similarly, most of these elongated RBCs break free from their points of contact, leaving behind small fragments adherent to the larger surface-associated RBC fragments, which we have termed rough bodies. The large and difficult-to-quantify number of endothelial blisters and rough bodies indicates the occurrence of in excess of thousands of transient RBC adhesion/dislocation events following FeCl$_3$ application.

It is interesting that we similarly observed elongated RBCs, RBC fragments, and RBC clusters in the carotid artery, mesenteric arterioles, and mesenteric venules, despite the marked shear rate differences among these vessel types ($\sim$1440 [s^{-1}], $\sim$1650 [s^{-1}], and $\sim$230 [s^{-1}], respectively).[11,15] Although the nature of the association between RBCs and the endothelial surface is unclear (ie, receptor mediated vs nonreceptor mediated), clearly this interaction must be of sufficient strength to mediate the binding of RBCs under conditions of arterial shear. In this regard, we found that FeCl$_3$ is able to induce the adhesion of washed human RBCs to cultured human endothelial cells in vitro (including the formation of RBC clusters), demonstrating that the interaction between RBCs and endothelial cells can occur directly, in the absence of soluble molecules. Consistent with this in vitro finding, we also demonstrated that FeCl$_3$-induced RBC adhesion does not require either VWF or GPIb-α in vivo.

As discussed above, the first study to describe FeCl$_3$-induced experimental thrombosis used SEM to characterize the resulting thrombotic material.[5] Interestingly, and again secondary to the quality of the available SEM imaging, Kurz et al[5] appear to have misidentified as aggregated platelets, in multiple images, what most likely are actually RBC fragments and rough bodies. Indeed, when reviewed in light of the results presented here, the images from this seminal report are completely consistent with our findings.

In addition to binding individually, circulating RBCs can also bind multiply to the FeCl$_3$-treated endothelial surface, frequently forming large multicellular clusters that are visible both by SEM and by intravital microscopy. When visualized by SEM, RBC clusters were observed to often be composed of rough and amorphous-appearing material that resembles the phenotypic appearance of rough bodies. Further imaging of multiple examples of RBC clusters revealed that this rough material represents elongated RBCs and RBC fragments in various stages of phenotypic change. Thus, as rough bodies derive from the adhesion points of adherent elongated RBCs, the rough material present in RBC clusters derives from RBC fragments and the elongated RBCs themselves.

The finding that rough bodies and rough material both derive from RBCs, coupled with their similar and distinctive appearances by SEM, suggests that these structures share a related mechanism of origin. Indeed, EDS imaging demonstrated both rough bodies and rough material to be strongly positive for iron content. Thus, we speculate that Fe ions present at the site of FeCl$_3$ application interact with adherent RBC fragments, resulting in the formation of rough bodies and rough material through an oxidative mechanism. In support of this notion, it was reported in 2009 that FeCl$_3$ is able to induce lipid peroxidation of RBCs in vitro.[14] Experiments are in progress to determine whether the rough appearance that is characteristic of rough bodies and rough material represents lipid peroxidation of RBC membranes.

Although the molecular nature of rough bodies and rough material remains to be determined, it is clear from both SEM and brightfield intravital imaging that these structures are responsible for recruiting platelets to the site of FeCl$_3$ application. Despite being present at an average concentration in mouse blood of

$\sim$1 $\times$ 10^6 cells per μL (approximately 10% of the circulating level of RBCs), only occasional platelets are observed to be directly adherent to the FeCl$_3$-treated endothelial surface. Rather, essentially all the platelets that are initially present at the site of FeCl$_3$ application are associated with RBC-derived structures, particularly rough bodies and the rough material present in RBC clusters. As discussed above, in 2011 Eckly et al[7] investigated FeCl$_3$-induced arterial thrombosis using SEM and TEM, and they identified structures similar to RBC fragments and rough bodies.[7] Eckly et al[7] also observed that platelets bound to these structures rather than to the endothelial surface, although these investigators believed the structures represent FeCl$_3$-containing exocytic bodies budding off from the endothelial surface. In the current study, we confirmed and extended this important finding by demonstrating that the material that mediates platelet binding following FeCl$_3$ application is derived from RBCs rather than from endothelial cells.

Regarding the nature of the association between platelets and RBC-derived structures, we found that the genetic deficiency of the platelet receptor GPIb-α greatly abrogated platelet-RBC binding. Interestingly, a similar effect was not observed in VWF-deficient mice, although VWF deficiency did abrogate the further recruitment of platelets to the already established platelet-RBC complexes, resulting in a slower rate of thrombus formation. Together, these findings demonstrate (1) a VWF-independent function of GPIb-α in mediating the association between platelets and RBC-derived material and (2) the existence of a GPIb-α ligand on potentially oxidized RBC membranes, which at this time we speculate may be oxidized RBC plasma membrane lipids.

These findings are consistent with the previous work Bergmeier et al[16] demonstrating a considerably greater role for GPIb-α compared with that of VWF in FeCl$_3$-induced arterial thrombosis. Interestingly, Bergmeier et al[16] demonstrated 2 distinct effects of GPIb-α deficiency in this model: (1) the inability of GPIb-α–deficient platelets to adhere to the site of injury (which was believed to represent the inability to adhere to the exposed subendothelial matrix) and (2) the inability of GPIb-α–deficient platelets to incorporate into an established thrombus composed of wild-type platelets. Regarding the former observation, it remained unclear why platelets deficient for GPIb-α (but sufficient for collagen receptors) were unable to adhere to the subendothelial matrix presumed to be exposed by FeCl$_3$ treatment. Our findings provided an answer to this question by demonstrating that GPIb-α deficiency results in the inability of platelets to bind to endothelial-associated RBC material rather than binding to subendothelial components (which are not actually exposed).

We observed that, following platelet recruitment to RBC-derived structures, thrombosis proceeds via continued platelet-platelet interactions (ie, platelet aggregation), likely explaining the sensitivity of the FeCl$_3$ model to a wide range of targeted gene deletions and antithrombotic agents (reviewed in Westrick et al,[1] Sachs and Nieswandt,[2] and Denis and Wagner[3]). However, secondary to our observation that the endothelial surface remains intact following FeCl$_3$ application, this model most likely is not appropriate for evaluating interventions intended to disrupt the association of platelets with the exposed subendothelium. This finding may explain the lack of a major phenotype for collagen receptor glycoprotein VI and integrin α2β1 deficiency observed in some studies.[7,17,18] However, for reasons that remain unclear, other investigators also have reported a severe thrombotic defect for glycoprotein VI deficiency in this model.[13,19]

Although they express multiple adhesion molecules, RBCs are not believed to be able to adhere to any other cell types under

normal physiological conditions.[20] However, there is a long-standing clinical observation that bleeding time is prolonged in anemic patients independent of platelet count, and that correction of the anemia by RBC transfusion improves both the bleeding time and clinical bleeding.[21-23] It has been postulated that RBCs promote hemostasis through a rheological effect displacing platelets closer to the endothelial surface during flow.[23] However, in light of our findings, it may be reasonable to investigate the possibility that RBCs can directly participate in hemostasis and thrombosis, especially under conditions of elevated intravascular oxidative stress or in patients with RBC abnormalities such as sickle cell anemia and paroxysmal nocturnal hemoglobinuria.

Acknowledgments

Authorship

Contribution: D.G.M. conceived and supervised the studies, interpreted the results, and wrote the manuscript. J.D.B., A.K.C., G.V.S, and J.K.H. performed the studies, interpreted the results, and contributed to the writing of the manuscript.

Conflict-of-interest disclosure: The authors declare no competing financial interests.

Correspondence: David Motto, MD, PhD, Departments of Internal Medicine and Pediatrics, 3269C CBRB, University of Iowa, Iowa City, IA 52242; e-mail: david-motto@uiowa.edu.

References

1. Westrick RJ, Winn ME, Eitzman DT. Murine models of vascular thrombosis (Eitzman series). *Arterioscler Thromb Vasc Biol.* 2007;27(10):2079-2093.

2. Sachs UJ, Nieswandt B. In vivo thrombus formation in murine models. *Circ Res.* 2007;100(7):979-991.

3. Denis CV, Wagner DD. Platelet adhesion receptors and their ligands in mouse models of thrombosis. *Arterioscler Thromb Vasc Biol.* 2007;27(4):728-739.

4. Owens AP III, Lu Y, Whinna HC, et al. Towards a standardization of the murine ferric chloride-induced carotid arterial thrombosis model. *J Thromb Haemost.* 2011;9(9):1862-1863.

5. Kurz KD, Main BW, Sandusky GE. Rat model of arterial thrombosis induced by ferric chloride. *Thromb Res.* 1990;60(4):269-280.

6. Ni H, Denis CV, Subbarao S, et al. Persistence of platelet thrombus formation in arterioles of mice lacking both von Willebrand factor and fibrinogen. *J Clin Invest.* 2000;106(3):385-392.

7. Eckly A, Hechler B, Freund M, et al. Mechanisms underlying FeCl3-induced arterial thrombosis. *J Thromb Haemost.* 2011;9(4):779-789.

8. Tseng MT, Dozier A, Haribabu B, et al. Transendothelial migration of ferric ion in FeCl3 injured murine common carotid artery. *Thromb Res.* 2006;118(2):275-280.

9. Denis C, Methia N, Frenette PS, et al. A mouse model of severe von Willebrand disease: defects in hemostasis and thrombosis. *Proc Natl Acad Sci USA.* 1998;95(16):9524-9529.

10. Kanaji T, Russell S, Ware J. Amelioration of the macrothrombocytopenia associated with the murine Bernard-Soulier syndrome. *Blood.* 2002;100(6):2102-2107.

11. Chauhan AK, Motto DG, Lamb CB, et al. Systemic antithrombotic effects of ADAMTS13. *J Exp Med.* 2006;203(3):767-776.

12. Megens RT, Reitsma S, Prinzen L, et al. In vivo high-resolution structural imaging of large arteries in small rodents using two-photon laser scanning microscopy. *J Biomed Opt.* 2010;15(1):011108.

13. Dubois C, Panicot-Dubois L, Merrill-Skoloff G, et al. Glycoprotein VI-dependent and -independent pathways of thrombus formation in vivo. *Blood.* 2006;107(10):3902-3906.

14. Woollard KJ, Sturgeon S, Chin-Dusting JP, et al. Erythrocyte hemolysis and hemoglobin oxidation promote ferric chloride-induced vascular injury. *J Biol Chem.* 2009;284(19):13110-13118.

15. Cheng C, Helderman F, Tempel D, et al. Large variations in absolute wall shear stress levels within one species and between species. *Atherosclerosis.* 2007;195(2):225-235.

16. Bergmeier W, Piffath CL, Goerge T, et al. The role of platelet adhesion receptor GPIbalpha far exceeds that of its main ligand, von Willebrand factor, in arterial thrombosis. *Proc Natl Acad Sci USA.* 2006;103(45):16900-16905.

17. Grüner S, Prostredna M, Schulte V, et al. Multiple integrin-ligand interactions synergize in shear-resistant platelet adhesion at sites of arterial injury in vivo. *Blood.* 2003;102(12):4021-4027.

18. Konstantinides S, Ware J, Marchese P, et al. Distinct antithrombotic consequences of platelet glycoprotein Ibalpha and VI deficiency in a mouse model of arterial thrombosis. *J Thromb Haemost.* 2006;4(9):2014-2021.

19. Massberg S, Gawaz M, Grüner S, et al. A crucial role of glycoprotein VI for platelet recruitment to the injured arterial wall in vivo. *J Exp Med.* 2003;197(1):41-49.

20. Cartron JP, Elion J. Erythroid adhesion molecules in sickle cell disease: effect of hydroxyurea. *Transfus Clin Biol.* 2008;15(1-2):39-50.

21. Anand A, Feffer SE. Hematocrit and bleeding time: an update. *South Med J.* 1994;87(3):299-301.

22. Boneu B, Fernandez F. The role of the hematocrit in bleeding. *Transfus Med Rev.* 1987;1(3):182-185.

23. Valeri CR, Khuri S, Ragno G. Nonsurgical bleeding diathesis in anemic thrombocytopenic patients: role of temperature, red blood cells, platelets, and plasma-clotting proteins. *Transfusion.* 2007;47(suppl 4):206S-248S.